Self-Terminating Protocol for an Interfacial Complexation Reaction *in Vacuo* by Metal–Organic Chemical Vapor Deposition

Anthoula C. Papageorgiou,[†,*] Sybille Fischer,[†] Seung Cheol Oh,[†] Özge Sağlam,[†] Joachim Reichert,[†,*] Alissa Wiengarten,[†] Knud Seufert,[†] Saranyan Vijayaraghavan,[†] David Écija,[†] Willi Auwärter,[†] Francesco Allegretti,[†,*] Robert G. Acres,[‡] Kevin C. Prince,[‡] Katharina Diller,[†] Florian Klappenberger,[†] and Johannes V. Barth[†]

[†]Physik Department E20, Technische Universität München, D-85748 Garching, Germany and [‡]Sincrotrone Trieste, Strada Statale 14, km 163.5, 34149 Basovizza, Trieste, Italy

ABSTRACT The fabrication and control of coordination compounds or architectures at well-defined interfaces is a thriving research domain with promise for various research areas, including single-site catalysis, molecular magnetism, light-harvesting, and molecular rotors and machines. To date, such systems have been realized either by grafting or depositing prefabricated metal–organic complexes or by protocols combining molecular linkers and single metal atoms at the interface. Here we report a different pathway employing metal–organic chemical vapor deposition, as exemplified by the reaction of *meso*-tetraphenylporphyrin derivatives on atomistically clean Ag(111) with a metal carbonyl precursor ($Ru_3(CO)_{12}$) under vacuum conditions. Scanning tunneling microscopy and X-ray spectroscopy reveal the formation of a *meso*-tetraphenylporphyrin cyclodehydrogenation product that readily undergoes metalation after exposure to the Ru-carbonyl precursor vapor and thermal treatment. The self-terminating porphyrin metalation protocol proceeds without additional surface-bound byproducts, yielding a single and thermally robust layer of Ru metalloporphyrins. The introduced fabrication scheme presents a new approach toward the realization of complex metal–organic interfaces incorporating metal centers in unique coordination environments.

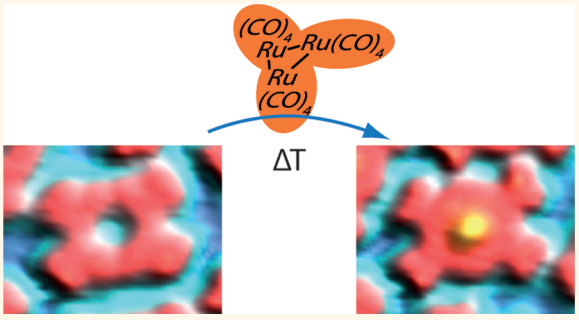

KEYWORDS: chemical vapor deposition · interfaces · monolayers · porphyrins · surface chemistry · silver surface

Surface coordination and organometallic systems attracted widespread attention in recent years, as they present prospects for single-site catalysis,[1–3] control and improvement of dye-sensitized solar cells,[4,5] or the engineering of interfacial metal–organic frameworks.[6,7] The coordination spheres of the embedded metal centers frequently present special features due to the influence of the underlying interface.[8–11] A series of interesting model systems could be realized regarding molecular magnetism,[12–15] molecular switches,[16–18] and molecular rotors.[19,20] To date, the fabrication schemes rely on the deposition of prefabricated species, by either solution techniques or sublimation (organic molecular beam epitaxy) or the co-deposition of metal atoms and molecular linkers at well-defined surfaces followed by complexation reactions.[10,21] Such reactions were notably explored using macrocyclic compounds, whereby the tetrapyrroles readily incorporate metal centers provided by atomic beams in ultrahigh vacuum (UHV). Hitherto this has been achieved by vacuum sublimation of solid metals (examples include Fe,[22–24] Co,[25,26] Zn,[27] Ni,[28] Ce,[19,29] and Cu[30]) or by directly capturing surface atoms (Cu,[31–34] Fe,[35] and Ni[35]). When targeting refractory or many other transition metals, the limitation of the former method is the high sublimation temperature of metals such as W, Ru, and Ir, whereas the latter is restricted to certain substrate materials. Here we consider the metal–organic chemical vapor deposition (MOCVD) approach for the metal–organic complexation and reactions at interfaces, which has the advantages of requiring minimal instrumentation and being applicable even outside vacuum.

* Address correspondence to a.c.papageorgiou@tum.de, francesco.allegretti@ph.tum.de, joachim.reichert@tum.de.

Received for review March 7, 2013 and accepted April 23, 2013.

Published online May 03, 2013
10.1021/nn401171z

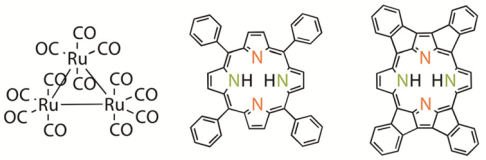

Figure 1. Molecular structures: metal precursor $Ru_3(CO)_{12}$ (1). The *meso*-tetraphenylporphyrin, 2H-TPP (2). The high-temperature 2H-TPP derivative on Ag(111) (3). Aminic (N1) and iminic (N2) N sites of the porphyrin macrocycle are indicated in green and orange, respectively.

Porphyrins provide model organic compounds whose physical and chemical properties depend sensitively on the choice of the metal center. The versatility of the macrocycle substituent further serves to tailor distinct structures and their interaction with surfaces and other molecules. In recent years, they have attracted considerable attention, finding application in catalysis (functionalization of saturated C−H bonds),[36] molecular electronics,[37] sensors,[38] and light-harvesting devices.[39,40] Ruthenium porphyrins in particular have been further applied to epoxidation and successfully tuned for enantio- and regioselectivity[41] as well as to cyclopropanation of alkenes *via* carbene complexes at the metal center.[42]

Trimetal dodecacarbonyls are organometallic compounds stable in air and labile by heat treatment. As such, they are regularly employed as metal precursors for chemical vapor deposition. In the study of model catalyst systems, they have been employed for the formation of metal clusters.[43] However, to the best of our knowledge, their potential in the synthesis of composite heterostructural materials engineered down to the atomic scale is hitherto unexplored. Earlier work hints that $Ru_3(CO)_{12}$ (Figure 1) is promising for well-defined reactions, as in solution porphyrins are known to react with it to yield Ru(CO) porphyrins[44] and it coordinates selectively with alkylamines.[45]

The *meso*-tetraphenylporphyrin **2** (2H-TPP, Figure 1) on the Ag(111) system is one of the most rigorously studied systems of large organic molecules on metal substrates. On the Ag(111) surface, its macrocycle has been shown to adopt a saddle shape conformation, whereas its phenyl legs exhibit a tilt angle of ∼50−55° with respect to the surface.[46] A recent study has revealed that, upon annealing to 550 K a multilayer of **2** in order to create a saturated monolayer, the molecule undergoes intramolecular cyclodehydrogenation reactions which result in a flat porphyrin.[47] Here we investigated the potential for metalation with the Ru precursor **1** on the thermally stable system of these high-temperature 2H-TPP derivatives (cf. Supporting Information Figure S1).

RESULTS AND DISCUSSION

Characterization of Metalation Substrate. A multilayer of **2** was grown onto a Ag(111) single crystal and was subsequently annealed to 550 K in order to form a saturated monolayer. The products of this temperature transformation of 2H-TPP on Ag(111) were identified by low-temperature (<160 K) scanning tunneling microscopy (STM) imaging: they include all possible cyclodehydrogenation products (Figure S1) proposed by di Santo *et al.*[47] but with a high selectivity toward porphyrin **3** (Figure 1) as the dominant product (Figure 2a). No extended close-packed islands were observed after such a heat treatment, whereas the actual porphyrin surface coverage decreased to 88% (±5%) as estimated by STM images. The corresponding angular-dependent near-edge X-ray absorption fine structure (NEXAFS) measurements are shown in Figure 2b along with the curve-fitting analysis to determine the angular orientation quantitatively (Figure 2c). The raw data at normal and grazing photon incidence are in excellent agreement with the ones reported previously for the high-temperature 2H-TPP derivative,[47] as the phenyl moieties of the molecule display a significantly reduced angle with respect to the surface plane (for the peak assignment, see Table S1).

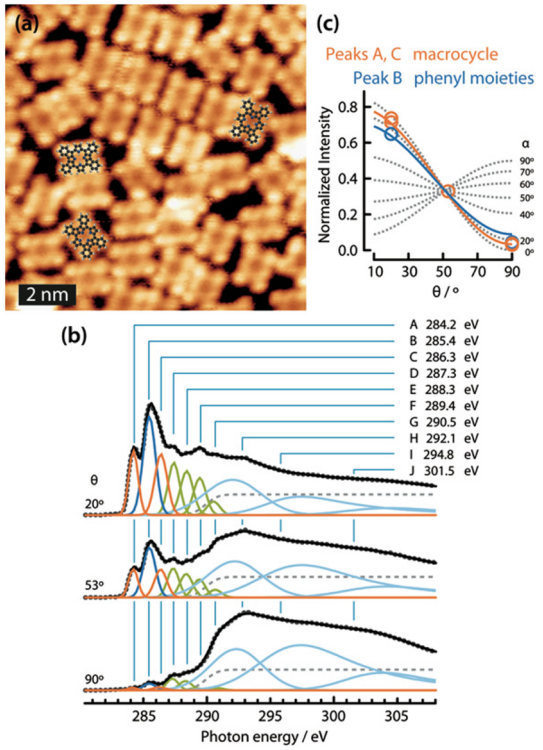

Figure 2. Characterization of cyclodehydrogenation products of 2H-TPP on Ag(111): (a) STM image (I = 0.5 nA, V_s = −1.4 V, 7 K) with superposed ball-and-stick representation of porphyrin 3. (b) Normalized experimental C K-edge NEXAFS data acquired at three angles of photon incidence, θ, and respective fit analysis. (c) Curve-fitting analysis of π^* resonances A, C, and B to estimate the tilt angles α (with respect to the Ag surface) of the macrocycle and the phenyl moieties of the molecule, respectively.

The corresponding N 1s signal (Figure 3a) shows two distinct peaks with almost equal intensity, which are located at 399.5 eV (component N1) and 397.9 eV

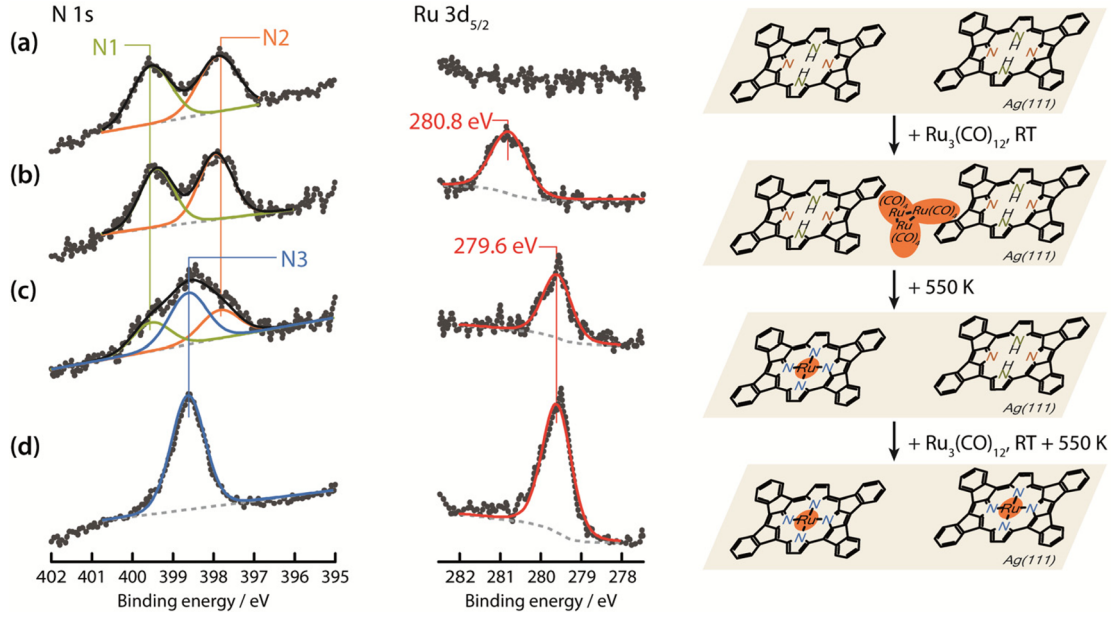

Figure 3. Sequential N 1s (left), Ru $3d_{5/2}$ (middle) core level spectra and corresponding cartoon (right) of the porphyrin Ru metalation process on Ag(111): (a) Layer of the flattened porphyrins on Ag(111) resulting from annealing a multilayer to ~550 K. (b) Following exposure leading to a saturated coverage of the Ru precursor at room temperature. (c) After annealing to ~550 K. (d) After further exposure leading to a saturated coverage of the Ru precursor at room temperature and annealing to ~550 K.

(component N2), corresponding to aminic and iminic N, respectively. These are shifted by ~0.6 and 0.2 eV, respectively, toward lower binding energy with respect to the peaks of the 2H-TPP (**2**),[25] a change which may be ascribed to electron transfer from the Ag substrate and/or to enhanced relaxation shift in the final state upon photoemission, both effects being most likely caused by the reduced distance between the macrocycle and the surface. The same trend is evident for the C 1s core level (Figure S2).[47] It can be seen that such transformations are evinced by XPS with relatively subtle differences, which are not fully understood. It is therefore emphasized that investigations of these porphyrin systems based solely on this technique may be inconclusive and moreover miss some essential points.

Porphyrin Metalation Process. After exposure of the Ag surface with the previously described layer of **3** at room temperature to the Ru precursor **1**, a saturation coverage of the latter accumulates without seemingly affecting the porphyrin overlayer. Further exposure of this surface to the Ru precursor did not change the Ru surface coverage, indicating a saturation coverage. Figure 3b shows that the N 1s signal (left column) still exhibits two peaks, despite the presence of Ru. Annealing the surface to 550 K (*i.e.*, a temperature at which the metal substrate does not cause any additional change in the porphyrin molecule) results in the transformation evidenced by the spectra reproduced in Figure 3c. A new component N3 at 398.6 eV is evident in the N 1s spectrum, its binding energy being typical of metalated porphyrins.[32] The N3 component coexists with N1 and N2, and its intensity is approximately equal to the sum of the intensities of N1 and N2, pointing to a layer where 50% of the porphyrin species are metalated. Concomitantly, the Ru $3d_{5/2}$ core level intensity decreases by ~16% due to either partial dissolution of Ru in the substrate or desorption of Ru molecular species. Moreover, the center of gravity of the peak shifts to 279.6 eV, which signifies metallic Ru.[48] The latter is somewhat unexpected given that if we consider a Ru porphyrin as a free molecule, the metal center has a nominal oxidation state of +2. The discrepancy with the detected oxidation state of Ru^0 is ascribed to charge transfer from the silver substrate. The same effect in the apparent oxidation state was observed also for Co-TPP[49] and Fe-phthalocyanine[3] in the contact layer with silver.

Additionally, no signal is detected in the O 1s region (Figure S2), thus proving the thermally activated scission accompanied by desorption of the carbonyl precursor ligands, which leaves the surface clean of reaction byproducts. As mentioned earlier, the reaction of porphyrins with $Ru_3(CO)_{12}$ in solution yields Ru porphyrins which are stabilized by axial ligation to carbonyl. However, it has been shown that axial ligands of porphyrin metal centers are not stable at high temperatures *in vacuo*; for example, Cl has been reported to dissociate from Mn(III)Cl porphyrin at 473 K,[50,51] NO dissociates from Co-TPP and Fe-TPP at 500 and 600 K, respectively,[9] whereas CO does not ligate with Co-TPP at room temperature.[8,11] In good accord with the temperature treatment of the molecular overlayer, carbonyl ligands are not detected for the metalated species.

The metalation is further confirmed by STM measurements. To our surprise, we found that the Ru

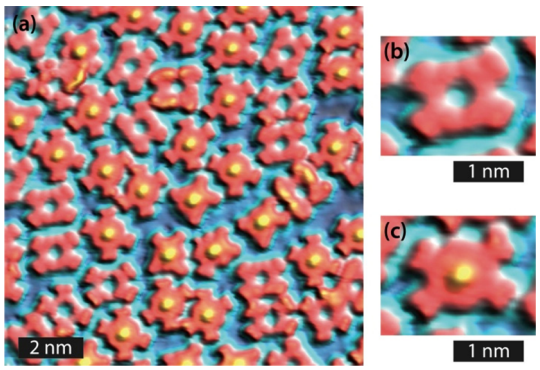

Figure 4. STM images of the Ru metalation of the cyclodehydrogenation products of 2H-TPP on Ag(111): (a) Overview (I = 0.2 nA, V_s = −0.5 V, 7 K). (b,c) Magnified images of a free base (b) and a metalated (c) porphyrin 3.

precursor is highly mobile on the surface or readily displaced by the presence of the STM tip even at the cryogenic temperature of ∼13 K. The presence of the Ru precursor dosed at room temperature on the Ag(111) surface is reflected by the induction of irregular step edges (cf. Figure S3a), whereas the morphology of the surface changes to clusters after annealing to ∼460 K (Figure S3b). Figure 4a shows a typical STM image probing the occupied states of the porphyrin layer after the metalation step with $Ru_3(CO)_{12}$. It is characterized by porphyrin molecules exhibiting either a depression (Figure 4b) or a protrusion (Figure 4c) in their center, depending on the occupation of the central cavity of the porphyrin macrocycle. In accordance with the valence band spectra which show a new energy state at ∼0.9 eV (Figure S4)[49,52] for the metalated porphyrin, the protrusions can be assigned to Ru centers. The absence of clusters and surface adsorbates other than porphyrins in the STM excludes metallic surface Ru outside the porphyrin macrocycle. The ratio of metalated to free base porphyrins in this STM experiment is found to be ∼3:2, which qualitatively agrees with the 1:1 ratio deduced from the XPS experiments above.

Additional exposure of this partially metalated porphyrin film to $Ru_3(CO)_{12}$ followed by annealing to 550 K as before leads to a fully metalated porphyrin layer: the N 1s signal now consists only of the N3 component (Figure 3d). It is noteworthy that the intensity ratio of the N3 components associated with the first and the second metalation steps is equal to the ratio of the corresponding Ru $3d_{5/2}$ intensities. Thus, there is a major and relatively unexpected advantage of using the trimetal dodecacarbonyl precursor for the metalation of this porphyrin layer, as the exposure did not need to be carefully controlled in an effort to avoid the formation of additional metal species on the surface. This is in contrast to the metalation strategy based on the direct deposition of metals *in vacuo*, which requires very precise control of the metal coverage in order to provide exactly a single metal atom for each molecule present on the surface. On the basis of the XPS data of the limited ruthenium surface accumulation, we therefore tentatively propose that the Ru precursor does not directly interact with the flat porphyrin at room temperature. Instead, it adsorbs at pristine metal patches, and the heat treatment is needed to activate its decomposition and entails the subsequent porphyrin complexation.

Conclusions and Future Prospects. In summary, we introduced a novel approach toward the engineering of interfacial coordination systems. Our multitechnique experimental study demonstrates the potential of metal−organic chemical vapor deposition to afford a robust layer with homogeneous composition, as exemplified by the realized metalated porphyrin films resulting from free base species exposed to gas-phase metal carbonyl precursors. With the particular system addressed, we also find that the reaction proceeds without build-up of surplus material and without any surface byproducts. Thus, a self-terminating protocol without the need of fine-tuning the exposure of the surface to the molecular reactants was developed for this interfacial metalation reaction. The method employed represents a versatile, facile, and convenient approach for implementing and addressing the functionality of a wide variety of metal centers and for the manufacturing of composite materials. Preliminary results of STM and XPS with three different porphyrins, namely the unmodified 2H-TPP (**2**), the flattened TPP (**3**) and the porphine, supported on Ag(111) show that metalation events with $Ru_3(CO)_{12}$ occur after annealing the porphyrin and metal precursor system to ∼500 K, thus demonstrating the wide applicability of the metalation process to other porphyrin species.

METHODS

XPS and NEXAFS experiments were carried out at the Materials Science beamline of the ELETTRA synchrotron light source in Trieste, Italy. The end station consists of a typical UHV surface science chamber, equipped with facilities for sample transfer, cleaning, dosing, and characterization and operated at a base pressure of 2×10^{-10} mbar. All measurements were performed with the sample kept at room temperature. Photoelectron spectra were collected using a SPECS PHOIBOS 150 electron energy analyzer of 150 mm mean radius and equipped with a nine-channel detector. The core levels were probed with photon energies of 435 (C 1s and Ru 3d), 550 (N 1s), and 680 eV (O 1s), and the binding energy scale was calibrated against the Ag $3d_{5/2}$ core level at 368.2 eV.[53] All photoelectron spectra shown were recorded in normal emission. The excitation energy for the acquisition of the valence band was 60 eV.

NEXAFS spectra were taken at the C K-edge using the carbon KVV Auger yield in three geometries: at normal (θ = 90°), at grazing (θ = 20°), and close to the magic angle geometry (θ = 53°) incidence of the photon beam with respect to the surface (Figure S5). The polarization of light from the beamline

has not been measured, but it is estimated to be between 80 and 90% linear, the radiation source being a bending magnet. The raw data were normalized to the relative intensity of the photon beam and divided by the corresponding spectrum of the clean substrate following established procedures.[54]

As the $Ru_3(CO)_{12}$ compound is reported to be light-sensitive,[44,55] in order to determine whether the porphyrin metalation is thermally or light activated, after the metalation step, we probed areas of the sample which had not been previously exposed to light. No difference was found, hence it was concluded that potential beam damage of the metal precursor is not critical for the porphyrin metalation, the latter being thermally activated.

STM measurements were carried out in two separate custom-made UHV systems with a CreaTec Fischer LT-STM operated at 7 K and an Aarhus 150 STM operated at 130−300 K. The base pressure during the experiments was $<2 \times 10^{-10}$ mbar in the LT-STM and $<1 \times 10^{-9}$ mbar in the Aarhus STM. All STM images were recorded in constant-current mode using electrochemically etched tungsten tips. V_s refers to sample bias. The WsXM program (www.nanotec.es) was used to display the STM images.

Ag(111) single-crystal surfaces (Surface Preparation Laboratory) were prepared by repeated cycles of Ar^+ sputtering and annealing until clean, atomically flat surfaces were obtained as monitored by XPS and low-energy electron diffraction (synchrotron measurements) or by STM. *meso*-Tetraphenylporphyrin (Sigma-Aldrich, ≥99%) was dosed by organic molecular beam epitaxy (vacuum sublimation temperature of 600−620 K) on the Ag(111) surface at room temperature. Triruthenium dodecacarbonyl (Aldrich, 99%) was dosed by exposure of the porphyrin film on Ag(111) to the vapor of the molecule at room temperature (Figure S6)[56] in a vacuum of $\sim 5 \times 10^{-8}$ mbar (Trieste) or $\sim 6 \times 10^{-10}$ mbar (Garching).

Conflict of Interest: The authors declare no competing financial interest.

Acknowledgment. Dr. Agustin Schiffrin is acknowledged for the application for beamtime. This work was supported by the ERC Advanced Grant MolArt (No. 247299), TUM-IAS, and the Munich Center for Advanced Phonics. A.C.P., Ö.S., and A.W. acknowledge support by a Marie Curie Intra-European Fellowship (Project NASUMECA, No. 274842), a Marie Curie International Incoming Fellowship (Project NANOULOP, No. 302157), and the International Max Planck Research School of Advanced Photon Science (IMPRS-APS), respectively. We thank our colleagues at Elettra for providing good quality synchrotron light. We thank Helmholtz-Zentrum Berlin (HZB) for the allocation of synchrotron radiation beamtime and financial support. Prof. Christof Wöll and Dr. Alexei Nefedov are acknowledged for support at the end station of the HE-SGM beamline, HZB.

Supporting Information Available: Molecular structures of all cyclodehydrogenation products of 2H-TPP on Ag(111); C K-edge peaks assignments; STM images of the Ag(111) after exposure to $Ru_3(CO)_{12}$; XP spectra of C 1s, Ru 3d, N 1s, and O1s; valence band spectra; schematic of NEXAFS setup; schematic of $Ru_3(CO)_{12}$ dosing setup. This material is available free of charge *via* the Internet at http://pubs.acs.org.

REFERENCES AND NOTES

1. Copéret, C. C−H Bond Activation and Organometallic Intermediates on Isolated Metal Centers on Oxide Surfaces. *Chem. Rev.* **2010**, *110*, 656–680.
2. Hulsken, B.; Van Hameren, R.; Gerritsen, J. W.; Khoury, T.; Thordarson, P.; Crossley, M. J.; Rowan, A. E.; Nolte, R. J. M.; Elemans, J. A. A. W.; Speller, S. Real-Time Single-Molecule Imaging of Oxidation Catalysis at a Liquid−Solid Interface. *Nat. Nanotechnol.* **2007**, *2*, 285–289.
3. Sedona, F.; Di Marino, M.; Forrer, D.; Vittadini, A.; Casarin, M.; Cossaro, A.; Floreano, L.; Verdini, A.; Sambi, M. Tuning the Catalytic Activity of Ag(110)-Supported Fe Phthalocyanine in the Oxygen Reduction Reaction. *Nat. Mater.* **2012**, *11*, 970–977.
4. Hagfeldt, A.; Boschloo, G.; Sun, L.; Kloo, L.; Pettersson, H. Dye-Sensitized Solar Cells. *Chem. Rev.* **2010**, *110*, 6595–6663.
5. Yella, A.; Lee, H.-W.; Tsao, H. N.; Yi, C.; Chandiran, A. K.; Nazeeruddin, M. K.; Diau, E. W.-G.; Yeh, C.-Y.; Zakeeruddin, S. M.; Grätzel, M. Porphyrin-Sensitized Solar Cells with Cobalt (II/III)-Based Redox Electrolyte Exceed 12% Efficiency. *Science* **2011**, *334*, 629–634.
6. Makiura, R.; Motoyama, S.; Umemura, Y.; Yamanaka, H.; Sakata, O.; Kitagawa, H. Surface Nano-architecture of a Metal−Organic Framework. *Nat. Mater.* **2010**, *9*, 565–571.
7. Shekhah, O.; Wang, H.; Paradinas, M.; Ocal, C.; Schupbach, B.; Terfort, A.; Zacher, D.; Fischer, R. A.; Wöll, Ch. Controlling Interpenetration in Metal−Organic Frameworks by Liquid-Phase Epitaxy. *Nat. Mater.* **2009**, *8*, 481–484.
8. Seufert, K.; Bocquet, M.-L.; Auwärter, W.; Weber-Bargioni, A.; Reichert, J.; Lorente, N.; Barth, J. V. *cis*-Dicarbonyl Binding at Cobalt and Iron Porphyrins with Saddle-Shape Conformation. *Nat. Chem.* **2011**, *3*, 114–119.
9. Hieringer, W.; Flechtner, K.; Kretschmann, A.; Seufert, K.; Auwärter, W.; Barth, J. V.; Görling, A.; Steinrück, H.-P.; Gottfried, J. M. The Surface Trans Effect: Influence of Axial Ligands on the Surface Chemical Bonds of Adsorbed Metalloporphyrins. *J. Am. Chem. Soc.* **2011**, *133*, 6206–6222.
10. Barth, J. V. Fresh Perspectives for Surface Coordination Chemistry. *Surf. Sci.* **2009**, *603*, 1533–1541.
11. Seufert, K.; Auwärter, W.; Barth, J. V. Discriminative Response of Surface-Confined Metalloporphyrin Molecules to Carbon and Nitrogen Monoxide. *J. Am. Chem. Soc.* **2010**, *132*, 18141–18146.
12. Wende, H.; Bernien, M.; Luo, J.; Sorg, C.; Ponpandian, N.; Kurde, J.; Miguel, J.; Piantek, M.; Xu, X.; Eckhold, P.; *et al.* Substrate-Induced Magnetic Ordering and Switching of Iron Porphyrin Molecules. *Nat. Mater.* **2007**, *6*, 516–520.
13. Wäckerlin, C.; Chylarecka, D.; Kleibert, A.; Müller, K.; Iacovita, C.; Nolting, F.; Jung, T. A.; Ballav, N. Controlling Spins in Adsorbed Molecules by a Chemical Switch. *Nat. Commun.* **2010**, *1*, 61.
14. Umbach, T. R.; Bernien, M.; Hermanns, C. F.; Krüger, A.; Sessi, V.; Fernandez-Torrente, I.; Stoll, P.; Pascual, J. I.; Franke, K. J.; Kuch, W. Ferromagnetic Coupling of Mononuclear Fe Centers in a Self-Assembled Metal-Organic Network on Au(111). *Phys. Rev. Lett.* **2012**, *109*, 267207.
15. Komeda, T.; Isshiki, H.; Liu, J.; Katoh, K.; Shirakata, M.; Breedlove, B. K.; Yamashita, M. Variation of Kondo Peak Observed in the Assembly of Heteroleptic 2,3-Naphthalocyaninato Phthalocyaninato Tb(III) Double-Decker Complex on Au(111). *ACS Nano* **2013**, *7*, 1092–1099.
16. Miyamachi, T.; Gruber, M.; Davesne, V.; Bowen, M.; Boukari, S.; Joly, L.; Scheurer, F.; Rogez, G.; Yamada, T. K.; Ohresser, P.; *et al.* Robust Spin Crossover and Memristance across a Single Molecule. *Nat. Commun.* **2012**, *3*, 938.
17. Mohn, F.; Repp, J.; Gross, L.; Meyer, G.; Dyer, M. S.; Persson, M. Reversible Bond Formation in a Gold-Atom−Organic-Molecule Complex as a Molecular Switch. *Phys. Rev. Lett.* **2010**, *105*, 266102.
18. Leoni, T.; Guillermet, O.; Walch, H.; Langlais, V.; Scheuermann, A.; Bonvoisin, J.; Gauthier, S. Controlling the Charge State of a Single Redox Molecular Switch. *Phys. Rev. Lett.* **2011**, *106*, 216103.
19. Écija, D.; Auwärter, W.; Vijayaraghavan, S.; Seufert, K.; Bischoff, F.; Tashiro, K.; Barth, J. V. Assembly and Manipulation of Rotatable Cerium Porphyrinato Sandwich Complexes on a Surface. *Angew. Chem., Int. Ed.* **2011**, *50*, 3872–3877.
20. Komeda, T.; Isshiki, H.; Liu, J.; Zhang, Y.-F.; Lorente, N.; Katoh, K.; Breedlove, B. K.; Yamashita, M. Observation and Electric Current Control of a Local Spin in a Single-Molecule Magnet. *Nat. Commun.* **2011**, *2*, 217.
21. Lin, N.; Stepanow, S.; Ruben, M.; Barth, J. V. Surface-Confined Supramolecular Coordination Chemistry. In *Templates in Chemistry III*, Broekmann, P., Dötz, K.-H., Schalley, C. A., Eds.; Springer: Berlin, 2009; Vol. 287, pp 1−44.

22. Auwärter, W.; Weber-Bargioni, A.; Brink, S.; Riemann, A.; Schiffrin, A.; Ruben, M.; Barth, J. V. Controlled Metalation of Self-Assembled Porphyrin Nanoarrays in Two Dimensions. *ChemPhysChem* **2007**, *8*, 250–254.
23. Écija, D.; Trelka, M.; Urban, C.; de Mendoza, P.; Mateo-Martí, E.; Rogero, C.; Martín-Gago, J. A.; Echavarren, A. M.; Otero, R.; Gallego, J. M.; *et al.* Molecular Conformation, Organizational Chirality, and Iron Metalation of *meso*-Tetramesitylporphyrins on Copper(100). *J. Phys. Chem. C* **2008**, *112*, 8988–8994.
24. Di Santo, G.; Castellarin-Cudia, C.; Fanetti, M.; Taleatu, B.; Borghetti, P.; Sangaletti, L.; Floreano, L.; Magnano, E.; Bondino, F.; Goldoni, A. Conformational Adaptation and Electronic Structure of 2H-Tetraphenylporphyrin on Ag(111) during Fe Metalation. *J. Phys. Chem. C* **2011**, *115*, 4155–4162.
25. Gottfried, J. M.; Flechtner, K.; Kretschmann, A.; Lukasczyk, T.; Steinrück, H.-P. Direct Synthesis of a Metalloporphyrin Complex on a Surface. *J. Am. Chem. Soc.* **2006**, *128*, 5644–5645.
26. Di Santo, G.; Sfiligoj, C.; Castellarin-Cudia, C.; Verdini, A.; Cossaro, A.; Morgante, A.; Floreano, L.; Goldoni, A. Changes of the Molecule−Substrate Interaction upon Metal Inclusion into a Porphyrin. *Chem.—Eur. J.* **2012**, *18*, 12619–12623.
27. Shubina, T. E.; Marbach, H.; Flechtner, K.; Kretschmann, A.; Jux, N.; Buchner, F.; Steinrück, H.-P.; Clark, T.; Gottfried, J. M. Principle and Mechanism of Direct Porphyrin Metalation: Joint Experimental and Theoretical Investigation. *J. Am. Chem. Soc.* **2007**, *129*, 9476–9483.
28. Chen, M.; Feng, X.; Zhang, L.; Ju, H.; Xu, Q.; Zhu, J.; Gottfried, J. M.; Ibrahim, K.; Qian, H.; Wang, J. Direct Synthesis of Nickel(II) Tetraphenylporphyrin and Its Interaction with a Au(111) Surface: A Comprehensive Study. *J. Phys. Chem. C* **2010**, *114*, 9908–9916.
29. Weber-Bargioni, A.; Reichert, J.; Seitsonen, A. P.; Auwärter, W.; Schiffrin, A.; Barth, J. V. Interaction of Cerium Atoms with Surface-Anchored Porphyrin Molecules. *J. Phys. Chem. C* **2008**, *112*, 3453–3455.
30. Li, Y.; Xiao, J.; Shubina, T. E.; Chen, M.; Shi, Z.; Schmid, M.; Steinrück, H.-P.; Gottfried, J. M.; Lin, N. Coordination and Metalation Bifunctionality of Cu with 5,10,15,20-Tetra(4-pyridyl)porphyrin: Toward a Mixed-Valence Two-Dimensional Coordination Network. *J. Am. Chem. Soc.* **2012**, *134*, 6401–6408.
31. González-Moreno, R.; Sánchez-Sánchez, C.; Trelka, M.; Otero, R.; Cossaro, A.; Verdini, A.; Floreano, L.; Ruiz-Bermejo, M.; García-Lekue, A.; Martín-Gago, J. Á.; *et al.* Following the Metalation Process of Protoporphyrin IX with Metal Substrate Atoms at Room Temperature. *J. Phys. Chem. C* **2011**, *115*, 6849–6854.
32. Diller, K.; Klappenberger, F.; Marschall, M.; Hermann, K.; Nefedov, A.; Wöll, Ch.; Barth, J. V. Self-Metalation of 2H-Tetraphenylporphyrin on Cu(111): An X-ray Spectroscopy Study. *J. Chem. Phys.* **2012**, *136*, 014705.
33. Nowakowski, J.; Wäckerlin, C.; Girovsky, J.; Siewert, D.; Jung, T.; Ballav, N. Porphyrin Metalation Providing an Example of a Redox Reaction Facilitated by a Surface Reconstruction. *Chem. Commun.* **2013**, *49*, 2347–2349.
34. Diller, K.; Klappenberger, F.; Allegretti, F.; Papageorgiou, A. C.; Fischer, S.; Wiengarten, A.; Joshi, S.; Seufert, K.; Écija, D.; Auwärter, W.; *et al.* Investigating the Molecule−Substrate Interaction of Prototypic Tetrapyrrole Compounds: Adsorption and Self-Metalation of Porphine on Cu(111). *J. Chem. Phys.* **2013**, *138*, 154710.
35. Goldoni, A.; Pignedoli, C. A.; Di Santo, G.; Castellarin-Cudia, C.; Magnano, E.; Bondino, F.; Verdini, A.; Passerone, D. Room Temperature Metalation of 2H-TPP Monolayer on Iron and Nickel Surfaces by Picking up Substrate Metal Atoms. *ACS Nano* **2012**, *6*, 10800–10807.
36. Che, C.-M.; Lo, V. K.-Y.; Zhou, C.-Y.; Huang, J.-S. Selective Functionalisation of Saturated C−H Bonds with Metalloporphyrin Catalysts. *Chem. Soc. Rev.* **2011**, *40*, 1950–1975.
37. Tour, J. M. Molecular Electronics. Synthesis and Testing of Components. *Acc. Chem. Res.* **2000**, *33*, 791–804.
38. Di Natale, C.; Salimbeni, D.; Paolesse, R.; Macagnano, A.; D'Amico, A. Porphyrins-Based Opto-electronic Nose for Volatile Compounds Detection. *Sens. Actuators, B* **2000**, *65*, 220–226.
39. Guldi, D. M. Fullerene-Porphyrin Architectures; Photosynthetic Antenna and Reaction Center Models. *Chem. Soc. Rev.* **2002**, *31*, 22–36.
40. Yu, J.; Mathew, S.; Flavel, B. S.; Johnston, M. R.; Shapter, J. G. Ruthenium Porphyrin Functionalized Single-Walled Carbon Nanotube Arrays—A Step toward Light Harvesting Antenna and Multibit Information Storage. *J. Am. Chem. Soc.* **2008**, *130*, 8788–8796.
41. Fackler, P.; Huber, S. M.; Bach, T. Enantio- and Regioselective Epoxidation of Olefinic Double Bonds in Quinolones, Pyridones, and Amides Catalyzed by a Ruthenium Porphyrin Catalyst with a Hydrogen Bonding Site. *J. Am. Chem. Soc.* **2012**, *134*, 12869–12878.
42. Che, C.-M.; Huang, J.-S. Ruthenium and Osmium Porphyrin Carbene Complexes: Synthesis, Structure, and Connection to the Metal-Mediated Cyclopropanation of Alkenes. *Coord. Chem. Rev.* **2002**, *231*, 151–164.
43. Kulkarni, A.; Lobo-Lapidus, R. J.; Gates, B. C. Metal Clusters on Supports: Synthesis, Structure, Reactivity, and Catalytic Properties. *Chem. Commun.* **2010**, *46*, 5997–6015.
44. Eaton, G. R.; Eaton, S. S. Reversible Carbon Monoxide Binding by Ruthenium Carbonyl Porphyrins. *J. Am. Chem. Soc.* **1975**, *97*, 235–236.
45. Chatani, N.; Asaumi, T.; Yorimitsu, S.; Ikeda, T.; Kakiuchi, F.; Murai, S. $Ru_3(CO)_{12}$-Catalyzed Coupling Reaction of sp^3 C−H Bonds Adjacent to a Nitrogen Atom in Alkylamines with Alkenes. *J. Am. Chem. Soc.* **2001**, *123*, 10935–10941.
46. Auwärter, W.; Seufert, K.; Bischoff, F.; Écija, D.; Vijayaraghavan, S.; Joshi, S.; Klappenberger, F.; Samudrala, N.; Barth, J. V. A Surface-Anchored Molecular Four-Level Conductance Switch Based on Single Proton Transfer. *Nat. Nanotechnol.* **2012**, *7*, 41–46.
47. Di Santo, G.; Blankenburg, S.; Castellarin-Cudia, C.; Fanetti, M.; Borghetti, P.; Sangaletti, L.; Floreano, L.; Verdini, A.; Magnano, E.; Bondino, F.; *et al.* Supramolecular Engineering through Temperature-Induced Chemical Modification of 2H-Tetraphenylporphyrin on Ag(111): Flat Phenyl Conformation and Possible Dehydrogenation Reactions. *Chem.—Eur. J.* **2011**, *17*, 14354–14359.
48. Wagner, C. D.; Riggs, W. M.; Davis, L. E.; Moulder, J. F.; Muilenberg, G. E. *Handbook of X-ray Photoelectron Spectroscopy: A Reference Book of Standard Data for Use in X-ray Photoelectron Spectroscopy*; Perkin-Elmer Corporation: Eden Prairie, MN, 1979.
49. Auwärter, W.; Seufert, K.; Klappenberger, F.; Reichert, J.; Weber-Bargioni, A.; Verdini, A.; Cvetko, D.; Dell'Angela, M.; Floreano, L.; Cossaro, A.; *et al.* Site-Specific Electronic and Geometric Interface Structure of Co-tetraphenyl-porphyrin Layers on Ag(111). *Phys. Rev. B* **2010**, *81*, 245403.
50. Turner, M.; Vaughan, O. P. H.; Kyriakou, G.; Watson, D. J.; Scherer, L. J.; Davidson, G. J. E.; Sanders, J. K. M.; Lambert, R. M. Deprotection, Tethering, and Activation of a Catalytically Active Metalloporphyrin to a Chemically Active Metal Surface: $[SAc]_4$P−Mn(III)Cl on Ag(100). *J. Am. Chem. Soc.* **2009**, *131*, 1910–1914.
51. Turner, M.; Vaughan, O. P. H.; Kyriakou, G.; Watson, D. J.; Scherer, L. J.; Papageorgiou, A. C.; Sanders, J. K. M.; Lambert, R. M. Deprotection, Tethering, and Activation of a One-Legged Metalloporphyrin on a Chemically Active Metal Surface: NEXAFS, Synchrotron XPS, and STM Study of [SAc]P−Mn(III)Cl on Ag(100). *J. Am. Chem. Soc.* **2009**, *131*, 14913–14919.
52. Fanetti, M.; Calzolari, A.; Vilmercati, P.; Castellarin-Cudia, C.; Borghetti, P.; Di Santo, G.; Floreano, L.; Verdini, A.; Cossaro, A.; Vobornik, I.; *et al.* Structure and Molecule−Substrate Interaction in a Co-octaethyl Porphyrin Monolayer on the Ag(110) Surface. *J. Phys. Chem. C* **2011**, *115*, 11560–11568.
53. Seah, M. P.; Gilmore, I. S.; Beamson, G. XPS: Binding Energy Calibration of Electron Spectrometers 5—Re-evaluation of the Reference Energies. *Surf. Interface Anal.* **1998**, *26*, 642–649.

54. Outka, D. A.; Stöhr, J. Curve Fitting Analysis of Near-Edge Core Excitation Spectra of Free, Adsorbed, and Polymeric Molecules. *J. Chem. Phys.* **1988**, *88*, 3539–3554.
55. Grevels, F. W.; Reuvers, J. G. A.; Takats, J. (.eta.2-Olefin)-tetracarbonylruthenium Complexes: Photochemical Syntheses from Dodecacarbonyltriruthenium and Quantum Yield Determinations. *J. Am. Chem. Soc.* **1981**, *103*, 4069–4073.
56. Cai, T.; Song, Z.; Chang, Z.; Liu, G.; Rodriguez, J. A.; Hrbek, J. Ru Nanoclusters Prepared by $Ru_3(CO)_{12}$ Deposition on Au(111). *Surf. Sci.* **2003**, *538*, 76–88.